

1 **MAXIMIZATION OF MONOMERIC C5 SUGARS FROM WHEAT**
2 **BRAN BY USING MESOPOROUS ORDERED SILICA**
3 **CATALYSTS**

4 Nuria Sánchez-Bastardo, Esther Alonso*

5 *Corresponding author: High Pressure Processes Group -Chemical Engineering and
6 Environmental Technology Department, C/Dr. Mergelina s/n, University of Valladolid, 47011,
7 Spain, +34 983 42 31 75, ealonso@iq.uva.es

8

9 **Abstract**

10 The hydrolysis process of real a fraction of arabinoxylans derived from wheat bran was studied
11 using different mesoporous silica materials and the corresponding RuCl_3 catalysts in water. The
12 influence of type and catalyst loading, reaction time and different metal cations were discussed
13 in terms of the hydrolysis yield of arabinose and xylose oligomers as well as the formation of
14 furfural as degradation product. A high yield of arabinoxylans into the corresponding
15 monomeric sugars (96 and 94% from arabino- and xylo-oligosaccharides, respectively) was
16 obtained at relatively high temperatures (180 °C) and short reaction times (15 min) with a
17 catalyst loading of 4.8 g of $\text{RuCl}_3/\text{Al-MCM-48}$ per g of initial carbon in hemicelluloses.

18 **Keywords:** arabinoxylan hydrolysis, wheat bran, biomass, heterogeneous catalysis, ruthenium
19 catalysts.

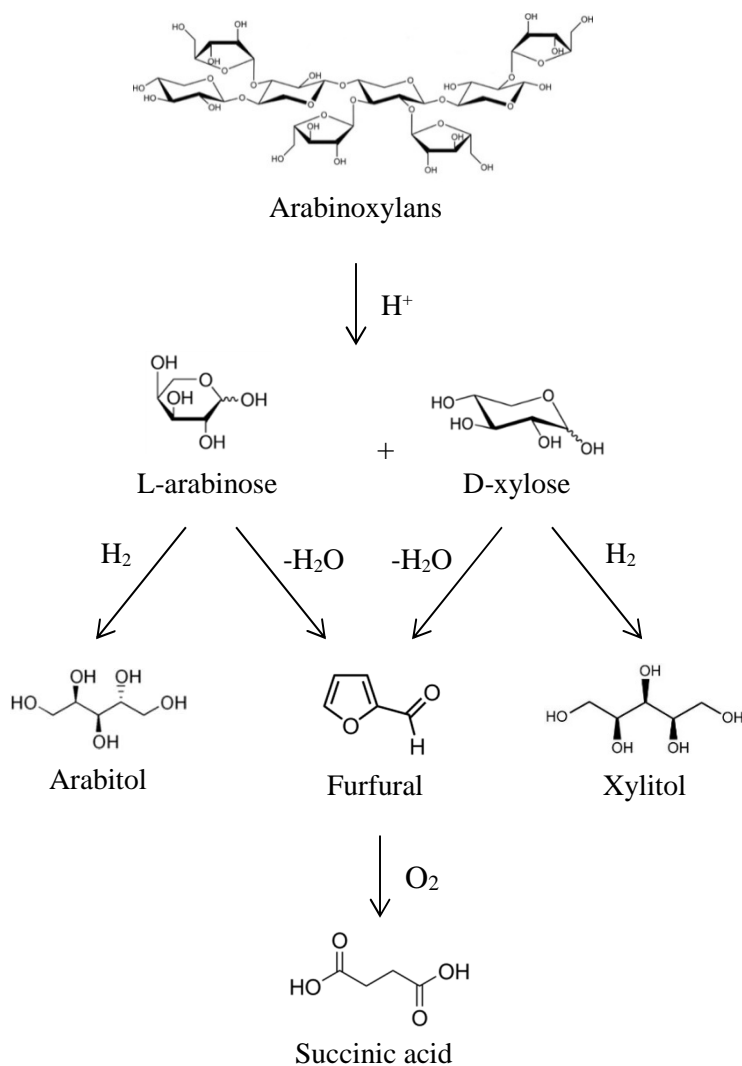
20 **Highlights:**

- 21 - $\text{RuCl}_3/\text{Al-MCM-48}$ is an active catalyst for arabinoxylan hydrolysis.
22 - $\text{RuCl}_3/\text{Al-MCM-48}$ accelerates conversion of arabinoxylans into arabinose and xylose.
23 - $\text{RuCl}_3/\text{Al-MCM-48}$ catalysts inhibit further dehydration into furfural.
24 - Significant reduction in hydrolysis time from several hours to 15 min is achieved.
25 - A two-step process using $\text{RuCl}_3/\text{Al-MCM-48}$ maximizes C5 sugars from wheat bran.

26 1. Introduction

27 The current depletion of fossil resources is forcing society to seek renewable alternatives for
28 energy and chemicals production. Biomass is considered a sustainable and renewable feedstock
29 to substitute fossil-based fuels (Negahdar et al., 2016; Oh et al., 2015; Putro et al., 2016;
30 Singhvi et al., 2014). Biomass accrues in large amounts all over the world as forestry and
31 agricultural waste. Moreover, around 95% of this biomass consists of lignocellulosic material
32 not edible for humans. Thus, its application to biofuels or chemicals synthesis does not compete
33 with food production (Negahdar et al., 2016; Sahu and Dhepe, 2012).

34 Agricultural residues like straw, corn stover or wheat bran appear as interesting feedstocks to
35 obtain high added-value products (Apprich et al., 2014). Wheat bran is a by-product of the
36 wheat grain milling. About 150 million tons are produced per year worldwide and its main use
37 is as a low value component in animal food (Prückler et al., 2014). The general composition of
38 wheat bran is as follows: water (12.1%), proteins (13.2 – 18.4%), fats (3.5 – 3.9%), starch (13.8
39 – 24.9%), cellulose (11.0%), arabinoxylans (10.9 – 26.0%), β -glucans (2.1 – 2.5%), phenolic
40 acids (0.02 – 1.5%) and ash (3.4 – 8.1%) (Apprich et al., 2014). Arabinoxylans (AXs) are a
41 major component contained in the cell walls of wheat bran. AXs belong to the hemicellulosic
42 part of biomass and are composed of a backbone of β -1,4 linked D-xylopyranosyl residues
43 (Izydorczyk and Biliaderis, 2007). The abundance of arabinoxylans in wheat bran makes them
44 susceptible to be extracted and converted into different platform molecules (furfural, succinic
45 acid, xylitol, arabitol, among others) (Apprich et al., 2014).



46

47 Fig. 1. Conversion of arabinoxylans into high added-value products (Choudhary et al., 2013;
 48 Kobayashi et al., 2011; Tathod et al., 2014; Zhang et al., 2012).

49 In general, hemicelluloses are partly solubilized and hydrolyzed during biomass fractionation,
 50 resulting in an aqueous fraction enriched in hemicellulosic poly/oligosaccharides and in a solid
 51 fraction with a high content in cellulose and lignin. Although hemicellulosic
 52 poly/oligosaccharides have important applications in pharmaceutical and food industries, the
 53 potential as platform molecules is larger for monomeric sugars. The reaction routes for the
 54 production of different chemicals from arabinoxylans are shown in Fig. 1. Arabitol, xylitol and
 55 succinic acid are found among the top 12 value-added products derived from biomass included
 56 in the report published by the US Department of Energy (DOE). For example, arabitol and
 57 xylitol are used as sugar substituents due to their low calorie content and also they are well

58 known for their anticariogenic properties (Koganti and Ju, 2013). Succinic acid has its main
59 application as a C4 building block for fuel additives, solvents and biopolymers, among others
60 (Choudhary et al., 2013).

61 Therefore, the fractionation and the complete hydrolysis of hemicellulosic poly/oligosaccharides
62 into monomers are critical for an integrated biorefinery. Fractionation implies the selectively
63 release of hemicelluloses from the biomass structure to the liquid medium. In a previous work, a
64 hydrothermal fractionation assisted by heterogeneous catalysts was used, and their conditions
65 were optimized (Sánchez-Bastardo et al., 2017). Hydrolysis of hemicelluloses is commonly
66 carried out by two different methods: using mineral acids (hydrolysis yield: 50-89%) (Hilpmann
67 et al., 2016; Kim et al., 2013; Kusema et al., 2013; Li et al., 2016; Nakasu et al., 2016) or
68 enzymes (hydrolysis yield: 6-84%) (Jia et al., 2016; Lee et al., 2013; Li, Wang et al., 2016; Li,
69 Xue et al., 2016; Lou et al., 2016; Moreira and Filho, 2016). Chemical hydrolysis using mineral
70 acids is not an environmentally-friendly process. Although the acids themselves are such a
71 cheap reagent, this process involves an increase in capital costs, as it requires corrosion resistant
72 materials. Moreover, a precipitation with calcium ions to remove the acid is needed, what
73 produces lime as a side product (Negahdar et al., 2016). The use of enzymes is a green process.
74 Nevertheless, the long time required (several hours and even days), the nonexistence of
75 recovery methods, the extremely high prize of enzymes and the critical control of reactions
76 make necessary to look for other alternatives (Aden et al., 2002; Cará et al., 2013; Hendriks and
77 Zeeman, 2009; Ormsby et al., 2012). Hydrolysis of hemicelluloses using solid acid catalysts
78 appears as a green alternative to these methods. Operation times can be reduced and
79 consequently the formation of degradation products and energy consumption. In the last 6 years,
80 the development of solid acid catalysts applied to hydrolysis processes of hemicelluloses has
81 attracted the interest of several authors (Cará et al., 2013; Dhepe and Sahu, 2010; Kusema et al,
82 2011; Sahu and Dhepe, 2012; Salmi et al., 2014; Vilcocq et al., 2014; Zhou et al., 2013).
83 Hydrolysis of polysaccharides over solid acid catalysts is a sequence of three first order
84 reactions: 1) hydrolysis of polysaccharides into oligosaccharides, 2) hydrolysis of

85 oligosaccharides into monosaccharides, 3) depending on the reaction conditions, dehydration of
86 monosaccharides into products such as furfural (Vilcocq et al., 2014). Different solid acid
87 catalysts have been tested for hemicelluloses hydrolysis: zeolites, sulfonated resins, mesoporous
88 silica materials, etc. Cará et al. (2013) reported a maximum hydrolysis yield of xylose +
89 arabinose of 80% using Amberlyst 35 as solid catalyst and commercial beechwood xylan as raw
90 material (120 °C, 10 bar argon, 4 hours). Dhepe et al. (2010) achieved a hydrolysis yield (xylose
91 + arabinose) equal to 54% from oat spelt using zeolite HUSY (Si/Al=15) (170 °C, 2 h, 50 bar
92 nitrogen). Kusema et al. (2011) used two different sulfonated resins to study the hydrolysis of
93 commercial arabinogalactan. The highest yield they reported was 95% (monomeric arabinose)
94 with Smopex-101 (pH=2) at 90 °C after 3 hours. Sahu et al. (2012) studied the effect of different
95 solid acid catalysts on the oat spelt hydrolysis. They got a hydrolysis yield (xylose + arabinose)
96 of 41% using zeolite HUSY (Si/Al=15) (170 °C, 3 h, 50 bar nitrogen). All these studies use
97 commercial hemicelluloses as model compounds of real hemicelluloses contained in different
98 types of biomass. However, only few studies are focused on the hydrolysis of hemicelluloses
99 extracted directly from biomass (Vilcocq et al., 2014). The process starts with the fractionation
100 of biomass to recover selectively the hemicellulosic fraction and complete the hydrolysis
101 subsequently. When hemicelluloses are extracted from real biomass, the purity of the extracts is
102 limited. Other compounds such as extractives, sugars, proteins and ash are also obtained
103 together with the hemicelluloses. All these compounds can interfere in the efficiency of the
104 hydrolysis process resulting in some limitations. Optimizing the hydrolysis step of a real
105 mixture enriched in hemicelluloses is an issue of utmost importance for a concept of a
106 biorefinery.

107 In this work, the heterogeneous catalytic hydrolysis of an extract enriched in arabinoxylans
108 obtained from destarched wheat bran has been studied. Different experimental conditions, such
109 as type and amount of catalyst and reaction time, have been tested in order to maximize the
110 yield into monomers (xylose and arabinose) and minimize their further degradation into
111 furfural.

112

113 2. Materials and Methods

114 2.1 Support and catalyst preparation

115 Synthesis of two mesoporous silica supports, MCM-48 and Al-MCM-48, was carried out using
116 the procedure described by Romero et al. in a previous work (Romero et al., 2016). 2.0 g of n-
117 hexadecyltrimethylammonium bromide (for molecular biology, $\geq 99\%$; Sigma-Aldrich) were
118 dissolved in 42 mL of distilled water, 18 mL of absolute ethanol (Panreac AppliChem) and 13
119 mL of an aqueous ammonia solution (20% w·w⁻¹) (Panreac AppliChem). After 15 minutes
120 stirring, 0.077 g of sodium aluminate (technical, anhydrous; Sigma-Aldrich) were incorporated
121 only for the Al-MCM-48 synthesis. Then, 4 mL of tetraethyl orthosilicate ($\geq 99.0\%$ (GC);
122 Sigma-Aldrich) were added dropwise and the solution was further stirred for 18 h. A white
123 precipitate was formed and recovered by filtration while washing with distilled water. This
124 precipitate was dried at 60 °C overnight. After drying, the samples were calcined to eliminate
125 the surfactant applying a heating rate of 2 °C·min⁻¹ from 80 to 550 °C and maintained at 550 °C
126 overnight.

127 Ruthenium or iron chloride catalysts were synthesized by wetness impregnation method using
128 the so prepared MCM-48 or Al-MCM-48 as silica supports (Romero et al., 2016). Ruthenium
129 (III) chloride (anhydrous; Strem Chemicals Inc.) or iron (III) chloride (reagent grade, 97%;
130 Sigma-Aldrich) together with the corresponding support were suspended in water and sonicated
131 for 10 minutes. This mixture was heated up from 30 to 80 °C with a heating rate of 1 °C·min⁻¹
132 and constant stirring. When water was evaporated, the resulting catalyst was dried overnight at
133 105 °C to eliminate the remaining water.

134 2.2 Support and catalyst characterization

135 Nitrogen adsorption-desorption isotherms were performed with ASAP 2020 (Micromeritics,
136 USA) to determine surface and pore properties of the catalysts. Before analysis, the samples
137 were outgassed overnight at 350 °C. The multipoint BET method at $P/P_0 \leq 0.3$ was used to
138 calculate the total specific surface area. The total specific pore volume was evaluated from N₂

139 uptake at $P/P_0 \geq 0.99$ and the pore diameter was determined by BJH adsorption average ($4 \cdot V \cdot A^{-1}$, nm).

141 The ruthenium amount of the RuCl_3 -based catalysts was determined by atomic absorption (AA)
142 spectrophotometry (SPECTRA 220FS analyser) after a digestion of the samples with HCl, H_2O_2
143 and HF using microwave at 250 °C.

144 The acidity of the different supports and metal catalysts was estimated by titration with NaOH.
145 This method is based on procedures already reported by several authors (Hu et al., 2015; Hu
146 et al., 2016; Liu et al., 2013; Wang et al., 2011; Zheng et al., 2014).

147 2.3 Recovery of arabinoxylan fraction from wheat bran

148 A destarched wheat bran suspension ($30 \text{ g} \cdot \text{L}^{-1}$) together with 500 mg of $\text{RuCl}_3/\text{Al-MCM-48}$ was
149 located in an extractor of 170 mL volume, made of AISI 304 stainless steel. The extraction was
150 performed at 180 °C and autogenous pressure for 10 minutes under hot compressed water
151 conditions. The optimization of these fractionation conditions is described in a previous work
152 (Sánchez-Bastardo et al., 2017). After cooling, the final mixture was filtered to separate the
153 remaining solid and the liquid extract enriched in arabinoxylans. This arabinoxylan extract,
154 composed mainly by oligomers, was further subjected to the hydrolysis process itself. The
155 composition of this extract that is indeed the raw material for the hydrolysis study is presented
156 in Table 1.

157 2.4 Hydrolysis experiments

158 Hydrolysis experiments of the extract enriched in arabinoxylans were performed in a
159 commercial stainless steel high pressure reactor (30 mL, Berghof BR-25) with a PID controller.
160 First, the corresponding solid catalyst was placed inside the reactor. Once the reactor was
161 closed, it was vented three times with nitrogen in order to eliminate the oxygen and heated up to
162 the operating temperature (180 °C). When desired temperature was reached, the arabinoxylan
163 solution preheated at 50 °C was pumped using a HPLC pump (PU-2080 Plus; Jasco). After
164 pumping, temperature inside the reactor dropped to approximately 170 °C and initial time (0
165 min) was considered when temperature reached again 180 °C (this lasts approximately 3 min).

166 At this moment, nitrogen pressure was adjusted to the operating pressure (50 bar). At the end of
167 the experiments, the reaction was quenched by introducing the reactor in an ice-bath. The
168 catalyst is recovered by filtration and the liquid was used for further analysis of monomeric
169 sugars, degradation products and by-products. The amount of catalyst in each experiment is
170 given as g of catalyst per g of C in initial hemicelluloses. However, in order to shorten, only g·g
171 C⁻¹ appears along the text.

172 2.5 Initial and final products analysis

173 The identification and quantification of sugars and degradation products were done by High
174 Performance Liquid Chromatography (HPLC).

175 The monosaccharides and degradation products were directly analyzed in the liquid samples.

176 However, for the total sugars determination in the initial solution (monomers and oligomers) an

177 acid hydrolysis pretreatment was used according to the Laboratory Analytical Procedure (LAP)

178 by NREL described by Sluiter et al. (2008). This method consisted of adding 0.8 mL of sulfuric

179 acid (72%) to 20 mL of the initial liquid sample. After the sample was autoclaved at 121 °C for

180 1 hour, calcium carbonate was added to get a pH between 5 and 6. An aliquot of 10 mL was

181 filtered (pore size 0.22 µm, Diameter 25 mm, Nylon; FILTER-LAB) and treated with 1 g of

182 mixed bed ion exchange resin (Dowex® Monosphere® MR-450 UPW; Sigma-Aldrich) to

183 remove all the ions before the HPLC analysis. All the samples were analyzed using a

184 chromatography system consisting of an isocratic pump (Waters 1515; Waters Corporation) and

185 an automatic injector (Waters 717; Waters Corporation). Two different HPLC columns were

186 used for the identification and quantification of the different products in the liquid samples:

187 1) Supelcogel Pb (Supelco) for sugars (milli-Q water as mobile phase, 0.5 mL·min⁻¹ as flow rate

188 and 85 °C as temperature) and 2) Sugar SH-1011 (Shodex) for degradation products (sulfuric

189 acid 0.01 N as mobile phase, 0.8 mL·min⁻¹ as flow rate and 50 °C as temperature). Sugars and

190 acids were identified using an IR detector (Waters 2414; Waters Corporation). 5-

191 hydroxymethylfurfural (5-HMF) and furfural were determined with an UV-Vis detector (Waters

192 2487; Waters Corporation) at a wavelength of 254 and 260 nm, respectively. The standards

193 employed for the HPLC analysis were: cellobiose (98%), glucose (99%), xylose (99%),
 194 galactose (99%), arabinose (99%), mannose (99%), fructose (99%), glyceraldehyde (95%),
 195 glycolaldehyde (99%), lactic acid (85%), formic acid (98%), acetic acid (99%), levulinic acid
 196 (98%), acrylic acid (99%), pyruvaldehyde (40%), 5-hydroxymethylfurfural (99%) and furfural
 197 (99%). All these chemicals were purchased from Sigma-Aldrich (Spain) and used as received.
 198 The hydrolysis yield of arabinose and xylose oligomers into arabinose and xylose, respectively,
 199 and the total arabinoxylan hydrolysis yield were calculated as follows (Eq. 1-3):

$$\% \text{ Ara hydrolysis yield} = \frac{\text{Ara as monomeric sugar in hydrolyzed liquid (g)}}{\text{Ara as total sugars}^a \text{ in initial liquid extract (g)}} \times 100 \quad (\text{Eq. 1})$$

$$\% \text{ Xyl hydrolysis yield} = \frac{\text{Xyl as monomeric sugar in hydrolyzed liquid (g)}}{\text{Xyl as total sugars}^a \text{ in initial liquid extract (g)}} \times 100 \quad (\text{Eq. 2})$$

$$\% \text{ AX hydrolysis yield} = \frac{(\text{Ara+Xyl}) \text{ as monomeric sugar in hydrolyzed liquid (g)}}{(\text{Ara+Xyl}) \text{ as total sugars}^a \text{ in initial liquid extract (g)}} \times 100 \quad (\text{Eq. 3})$$

200 Ara: Arabinose, Xyl: Xylose

201 ^a Total sugars refer to the sum of the corresponding sugars (arabinose and/or xylose) as monomers plus
 202 oligomers

203 3. Results and Discussion

204 3.1 Composition of initial arabinoxylan extract

205 The composition of the enriched arabinoxylan extract obtained from wheat bran and used in the
 206 hydrolysis experiments is given in Table 1. Table 1 presents the amount of each sugar which is
 207 in monomeric and oligomeric form respect the total amount of the corresponding sugar. In the
 208 case of arabinose, practically 50% percent is already in monomeric form after the fractionation
 209 process, whereas 95% of the xylose appears as oligosaccharide.

210 The initial total amount of arabinose and xylose (monomers + oligomers) expressed in g·L⁻¹ is
 211 3.1 and 6.2, respectively. This means that these are the maximum values which both sugars can
 212 reach after the hydrolysis process.

213

214

215 Table 1. Chemical composition of the initial extract.

Compound			
Proteins ^a (mg/L)	1676 ± 113		
Sugars	Monomeric sugars (mg/L)	Oligomeric sugars (mg/L)	% Olig ^b
Glc	195 ± 32	1609 ± 197	89
Xyl	284 ± 9	5944 ± 188	95
Gal	82 ± 26	255 ± 34	76
Ara	1522 ± 112	1605 ± 34	51
Man	70 ± 9	2 ± 44	2

216 ^a Proteins were determined following a standardized Kjeldahl method using a nitrogen to protein conversion factor of
217 5.7 applicable to wheat bran

218 ^b %Olig. = percentage of each sugar in oligomeric form: g of each oligomeric sugar/g of the total corresponding sugar
219 x 100

220 3.2 Catalyst characterization

221 The properties of the different solid catalysts used in this work are summarized in Table 2.

222 Specific surface area, total pore volume, pore diameter and acidity values were determined.

223 MCM-48 and Al-MCM-48 have specific surface areas of 1298 and 1352 m²·g⁻¹, and pore

224 volumes of 0.87 and 0.81 cm³·g⁻¹, respectively. According to these results, no significant

225 changes in surface area and pore volume were observed between these two mesoporous

226 materials. Pore diameter was slightly higher for Al-MCM-48 (2.5 nm) than for MCM-48 (2.2

227 nm). After RuCl₃ or FeCl₃ impregnation, a decrease in the specific surface area and pore volume

228 was detected. This fact can be attributed to the partial blocking of the porous network in

229 mesoporous supports. After RuCl₃ deposition on MCM-48, no changes in the pore size were

230 appreciated. However, pore size slightly increased from 2.5 to 2.7 nm and 2.6 nm after

231 deposition of RuCl₃ and FeCl₃, respectively, on Al-MCM-48. This indicates slender

232 modifications of pore structure, suggesting a higher pore blocking in Al-MCM-48 supported

233 catalysts than in MCM-48 catalysts. Ruthenium and iron content for RuCl₃ and FeCl₃-based

234 catalysts was around 4% in both cases, determined by AA.

235 Acidity is a key parameter of catalysts for hydrolysis reactions. The acidity of the catalysts used

236 in this work presents the following trend: MCM-48 < Al-MCM-48 < RuCl₃/MCM-48 <

237 RuCl₃/Al-MCM-48 < FeCl₃/Al-MCM-48.

238 Table 2. Structural characterization of solid catalysts.

Catalyst	Metal content (%)	S _{BET} (m ² ·g ⁻¹)	V _{pore} ^a (cm ³ ·g ⁻¹)	D _{pore} ^b (nm)	Acidity (mEq H ⁺ ·g cat. ⁻¹)
MCM-48	-	1298	0.87	2.2	0.293
Al-MCM-48	-	1352	0.81	2.5	0.598
RuCl ₃ /MCM-48	4.1	1032	0.63	2.2	0.738
RuCl ₃ /Al-MCM-48	4.3	1018	0.63	2.7	1.130
FeCl ₃ /Al-MCM-48	4.2	1018	0.59	2.6	1.429

239 ^a Total specific pore volume was evaluated from N₂ uptake at $P/P_0 \geq 0.99$

240 ^b Pore diameter was determined by BJH adsorption average

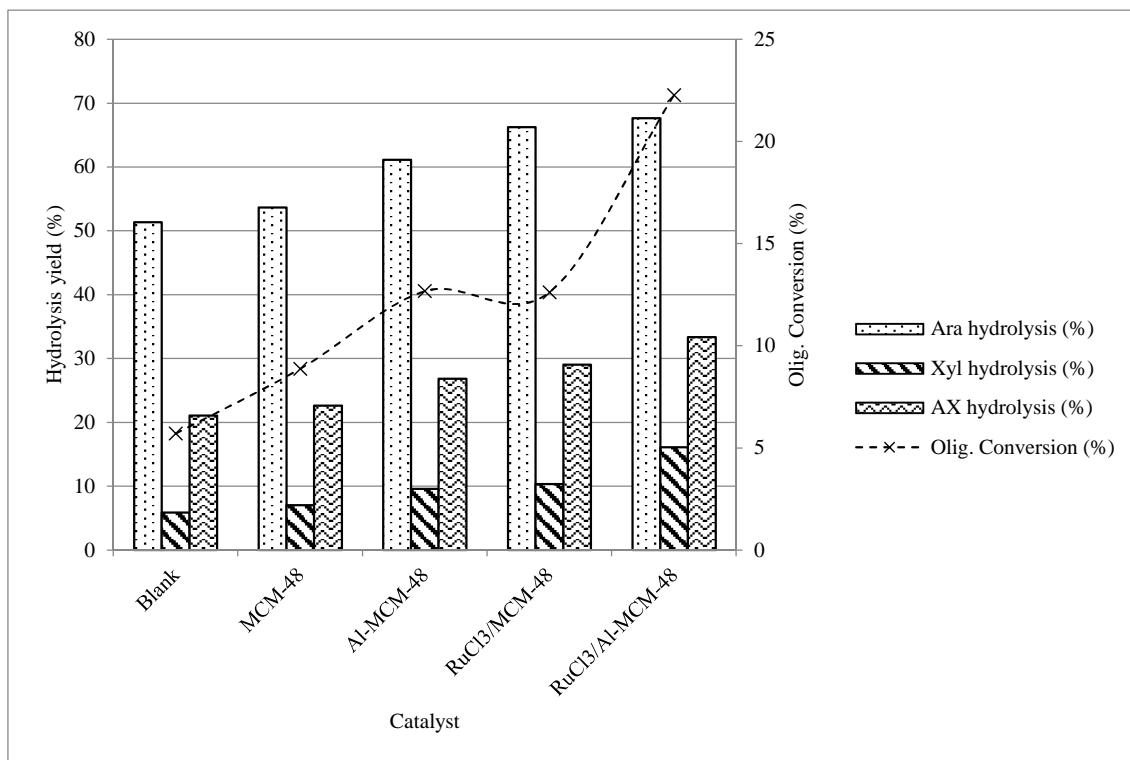
241 3.3 Arabinoxylan hydrolysis experiments

242 The effect of different parameters (type and amount of catalyst, reaction time and different
 243 metal cations) was studied in the hydrolysis of an arabinoxylan enriched extract obtained from
 244 destarched wheat bran. The results are discussed in terms of hydrolysis yield of arabinose and
 245 xylose oligomers. The formation of furfural, as the main degradation product derived from
 246 dehydration of arabinose and xylose, was also taken into account.

247 3.3.1 Effect of different mesoporous silica materials and RuCl₃ based-catalysts

248 A first screening of different mesoporous silica supports and the corresponding RuCl₃ based-
 249 catalysts was carried out. MCM-48, Al-MCM-48, RuCl₃/MCM-48 and RuCl₃/Al-MCM-48 were
 250 tested in the arabinoxylan hydrolysis (Fig. 2). The experimental conditions were 180 °C, 15
 251 minutes and 50 bar N₂. The ratio of catalyst to carbon content in hemicelluloses of the initial
 252 extract was 0.6 g·g⁻¹, which is the same ratio used in the previous fractionation from wheat bran.
 253 The trend observed in total AX hydrolysis yield is as follows: Blank \approx MCM-48 < Al-MCM-48
 254 < RuCl₃/MCM-48 < RuCl₃/Al-MCM-48. This is in agreement with the acidity values of
 255 catalysts: higher acidities result in higher hydrolysis yields. In the absence of catalyst (blank
 256 reaction), the amount of monomeric arabinose and xylose turns out to be the same as in the
 257 initial AX solution (Table 1). At 180 °C, the pK_w of water is low, which means that the amount
 258 of protons derived from water is relatively high (Bandura and Lvov, 2006). However, as it is
 259 shown in Fig. 2, the water protonation is not enough to cause the breakdown of arabinoxylan
 260 molecules into monomers under these conditions. MCM-48 is the least acidic catalyst and its
 261 surface acidity is due to silanol groups (Si – OH), which correspond to weak acid sites (Xue et.,

262 2004). The weak nature of these sites does not practically improve AX hydrolysis, although a
263 slight increase in arabinose oligomers hydrolysis is observed. Al-MCM-48 exhibits a higher
264 catalytic activity in this hydrolysis process. Specially, Al-MCM-48 improves the conversion of
265 arabinose oligomers into monomers. During Al-MCM-48 synthesis, a silicon atom (Si^{+4}) is
266 replaced by an aluminum atom (Al^{+3}) in a tetrahedral network. Thus, a cation, usually a proton,
267 is required to balance the aluminum tetrahedron. This compensation proton derives in a
268 Brønsted acid site, which increases the total acidity of the Al-MCM-48 (Kao et al., 2008). In Al-
269 MCM-48, Brønsted acidity is higher than Lewis acidity due to the large amount of
270 tetraordinated aluminum on the silica surface (Krithiga et al., 2005). RuCl_3 supported
271 catalysts ($\text{RuCl}_3/\text{MCM-48}$ and $\text{RuCl}_3/\text{Al-MCM-48}$) demonstrated to be more active in AXs
272 hydrolysis than the corresponding mesoporous silica materials (MCM-48 and Al-MCM-48,
273 respectively). Higher activity of RuCl_3 catalysts in hydrolysis reactions is related to their global
274 acidity. RuCl_3 -based catalysts show higher acidity than the corresponding mesoporous silica
275 support, which is due to the high acidity of RuCl_3 (Guisnet et al., 1993). In addition to this,
276 several authors have already reported that cations with moderate Lewis acidity, such as Ru^{+3} ,
277 are found to be active in hydrolysis of cellobiose or cellulose (Jing et al., 2016; Shimizu et al.,
278 2009). In all the cases, furfural formation was negligible in comparison to the amount of
279 arabinose and xylose.



280

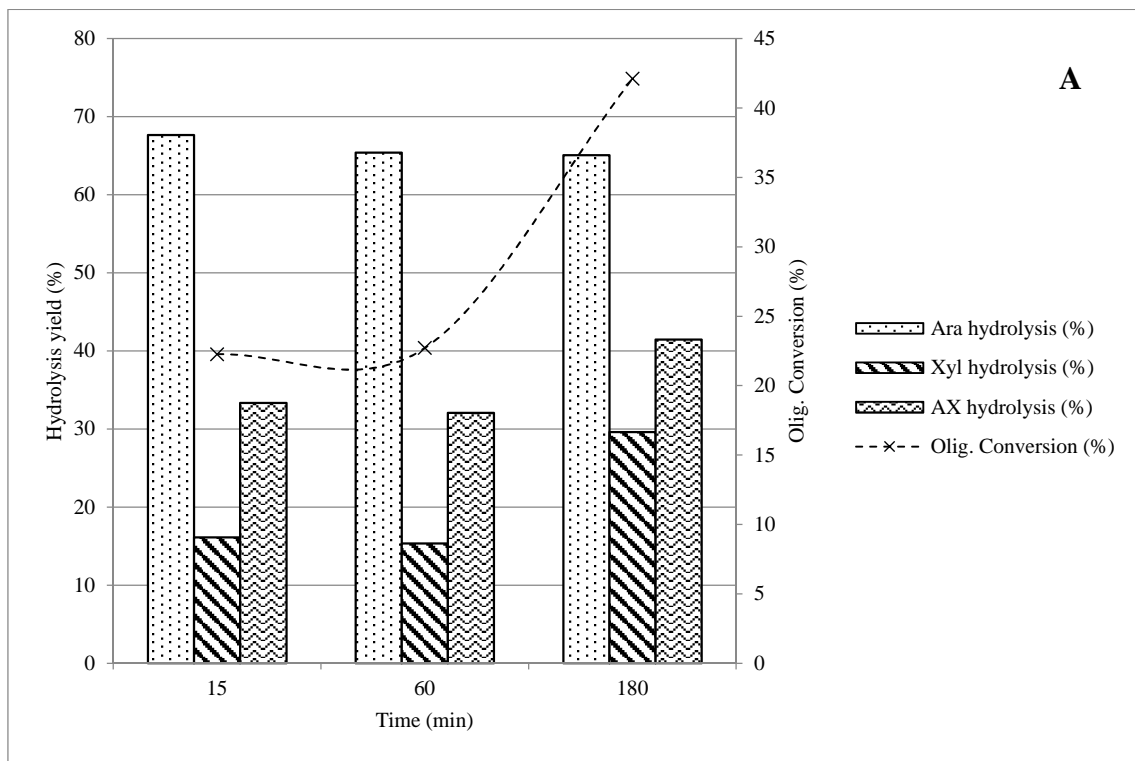
281 Fig. 2. Comparison of different catalysts in arabinoxylan hydrolysis yield and oligomers
 282 conversion. Reaction conditions: 180 °C, 50 bar N₂, 15 min, 0.6 g catalyst·g C⁻¹ in initial
 283 hemicelluloses.

284 Although it has been shown that a more acidic catalyst leads to a higher conversion of AXs into
 285 monomeric sugars, hydrolysis yields and oligomer conversion under these experimental
 286 conditions were still very low. RuCl₃/Al-MCM-48, as the most active catalyst, was chosen for a
 287 further study to improve hydrolysis yield.

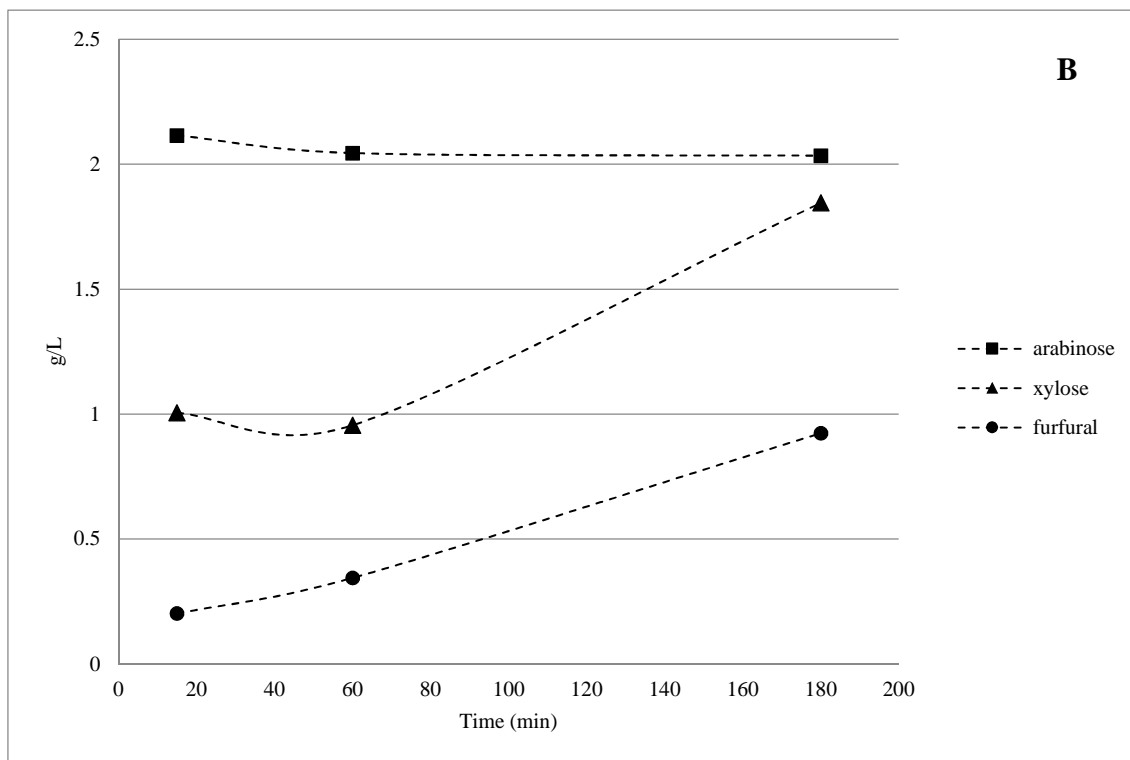
288 3.3.2 Effect of catalyst amount and reaction time

289 RuCl₃ supported on mesoporous Al-MCM-48 was used to study the influence of reaction time
 290 and catalyst loading on hydrolysis yield. First, a low amount of catalyst (0.6 g·g C⁻¹) was tested
 291 at 180 °C, 50 bar N₂ and different reaction times (15-180 min) (Fig. 3). A maximum of 68% in
 292 the hydrolysis yield of arabinose oligomers is achieved at 15 minutes of reaction, as a
 293 consequence of their degradation into furfural for longer times. No difference is observed in
 294 terms of arabino-oligosaccharides hydrolysis yield for times beyond 15 minutes. However, with
 295 this low amount of catalyst, the maximum hydrolysis yield of xylose oligomers is obtained after

296 180 minutes of reaction, where the concentration of furfural becomes also important due to
 297 xylose degradation, as it is shown in Fig. 3B. This means that monomeric xylose is slowly
 298 formed and partially degraded into furfural after 3 hours. Part of xylose obtained over time has
 299 had probably enough time to be converted into furfural. At short times, xylose detected is low
 300 because xylose oligomers have not been hydrolyzed. At longer times, this amount is higher but
 301 hydrolysis yield of xylose oligomers is still low ($\approx 30\%$) due to the slow xylose formation from
 302 xylo-oligosaccharides and fast degradation into furfural. The large quantity of furfural also
 303 evidences the slow hydrolysis rate of xylose oligomers into xylose compared to the high
 304 degradation rate of xylose into furfural.



305

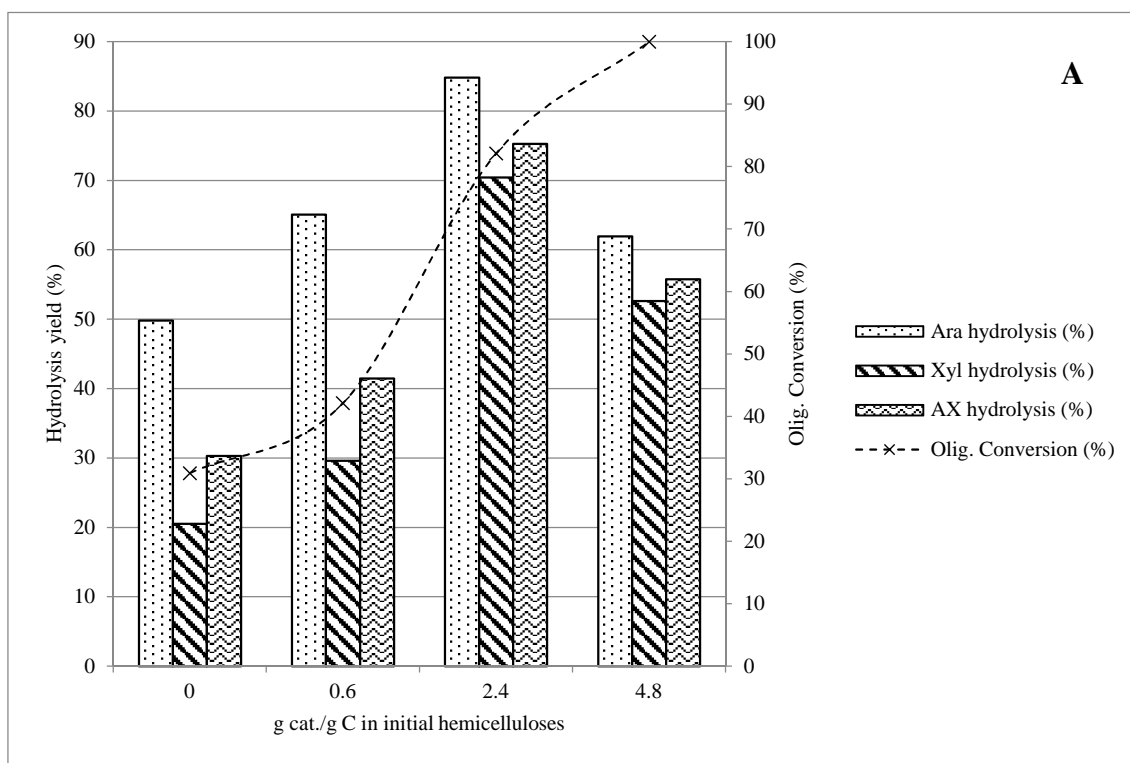


306

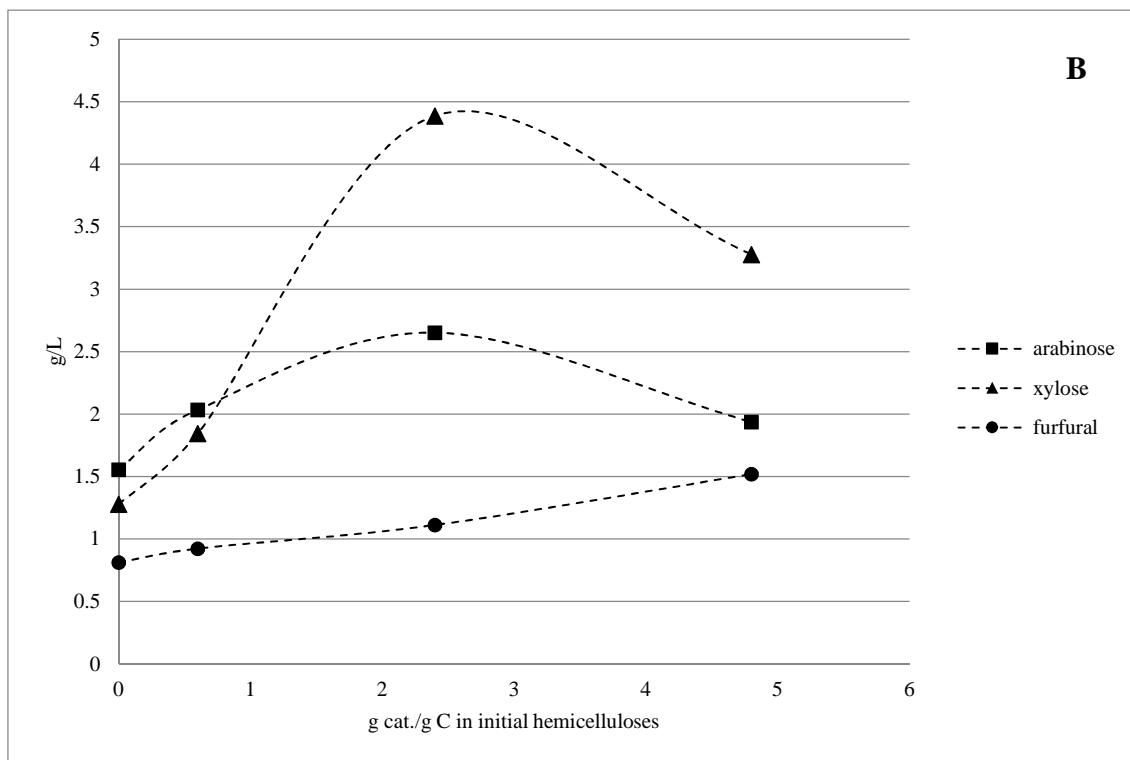
307 Fig. 3. Effect of time in arabinoxylan hydrolysis with low amount of catalyst. Reaction
 308 conditions: 180 °C, 50 bar N₂, catalyst: RuCl₃/Al-MCM-48, catalyst loading: 0.6 g catalyst·g C⁻¹
 309 in initial hemicelluloses. A) Hydrolysis yield and oligomers conversion, B) Composition of the
 310 liquid after hydrolysis (g·L⁻¹).

311 To overcome this degradation is necessary to speed up the xylo-oligosaccharides hydrolysis step
 312 but inhibiting further degradation. Three different amounts of catalyst (0.6, 2.4 and 4.8 g·g C⁻¹)
 313 were tested at 180 °C and 3 hours under 50 bar of N₂ (Fig. 4). The hydrolysis yield of xylose
 314 oligomers reaches 70% after 3 hours with a catalyst loading of 2.4 g·g C⁻¹. Under these
 315 conditions, the hydrolysis yield of arabino-oligosaccharides is already 85%. When catalyst
 316 loading is increased from 0.6 to 2.4 g·g C⁻¹, monomeric xylose and arabinose in the liquid after
 317 hydrolysis rise in a greater proportion than furfural. This means that arabinose and xylose
 318 formation is faster than the consecutive degradation into furfural. This was also observed and
 319 well explained by Sahu et al. (2012). They studied the effect of substrate/catalyst ratio on
 320 hemicelluloses hydrolysis using HUSY zeolite as catalyst. Interactions between the substrate
 321 (hemicelluloses) and available active sites in catalyst decrease as increasing substrate/catalyst

322 ratio (decreasing catalyst amount); in addition to this, once xylose is formed, it may undergo
 323 non-catalytic degradation reactions. In that work, a xylose+arabinose yield of 35% was reported
 324 when substrate/catalyst ratio was 130. However, when this ratio was 10, the yield of
 325 arabinose+xylose was 56%. They concluded that the reaction rate of hemicelluloses into xylose
 326 was higher than xylose to furfural when the amount of catalyst was increased. In the present
 327 work, when catalyst loading was further increased (from 2.4 to 4.8 g·g C⁻¹), the oligomer
 328 conversion was total. However, after 3 hours of hydrolysis, a dramatic decrease in xylose and
 329 arabinose is observed and black sediment appears. This black sediment corresponds probably to
 330 humins derived from furfural: arabinose and xylose are degraded to furfural and this later to
 331 humins; that explains a drop in arabinose and xylose but not a sharp increase in furfural as it is
 332 shown in Fig. 4B.



333

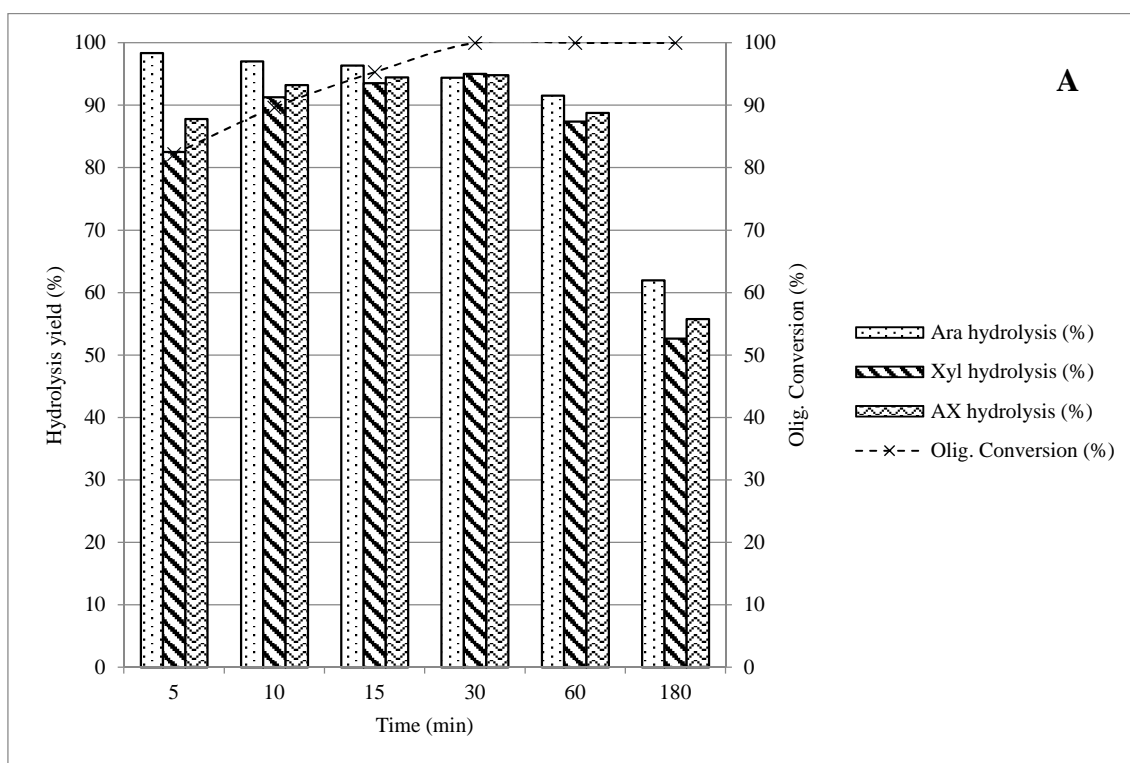


334

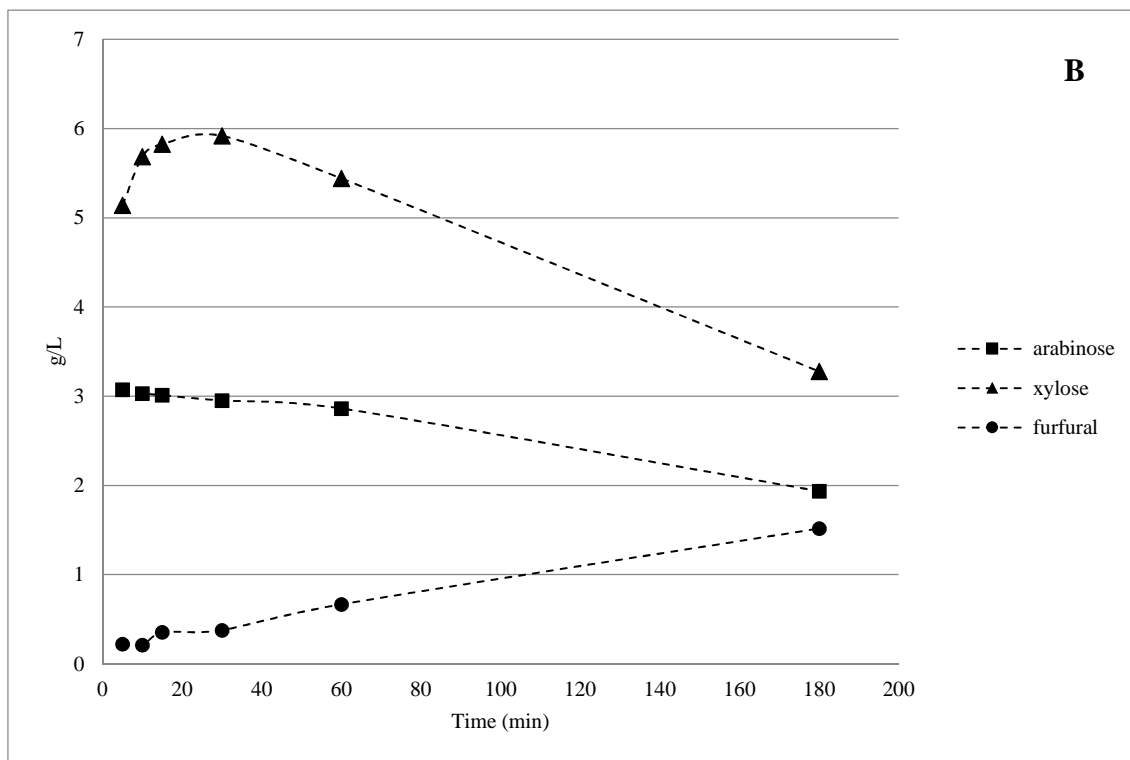
335 Fig. 4. Effect of the amount of catalyst in arabinoxylan hydrolysis. Reaction conditions: 180 °C,
 336 3 h, 50 bar N₂, catalyst: RuCl₃/Al-MCM-48. A) Hydrolysis yield of arabinoxylans and
 337 oligomers conversion, B) Composition of the liquid after hydrolysis (g·L⁻¹).

338 In order to shorten reaction times and subsequent degradation, the highest catalyst loading (4.8
 339 g·g C⁻¹) was tested at shorter times (< 180 min) (Fig. 5). The hydrolysis yield of arabinose
 340 oligomers is almost complete after 5 minutes (98%). Longer times make arabinose degrade
 341 slowly into furfural. The hydrolysis of xylose oligomers gets the maximum yield after 15-30
 342 minutes (94-95%), and then xylose starts to be degraded. Total conversion of oligomers is
 343 reached after 15 minutes. The amount of furfural obtained rises after 30 minutes, due to
 344 arabinose and xylose degradation. The hydrolysis of arabinose oligomers is always higher than
 345 that of xylose. Arabinose side chains are linked by α-glycosidic bonds, whereas xylose units
 346 from the backbone are connected by means of β-glycosidic bonds. α-glycosidic bonds are more
 347 easily hydrolysable than β-glycosidic linkages, what explains the faster release of arabinose
 348 molecules than xylose. This is well reported by Negahdar et al. (2016).

349 In conclusion, a high arabinoxylan hydrolysis yield was achieved at 180 °C, 15 minutes and 50
350 bar N₂ with a catalyst loading of 4.8 g·g C⁻¹. Arabinose and xylose oligomers hydrolysis yields
351 were 96 and 94%, respectively. Under these conditions, the process is optimized since xylose
352 and arabinose reach practically the maximum amount possible. Moreover, the amount of
353 furfural was negligible in comparison to arabinose and xylose.



354



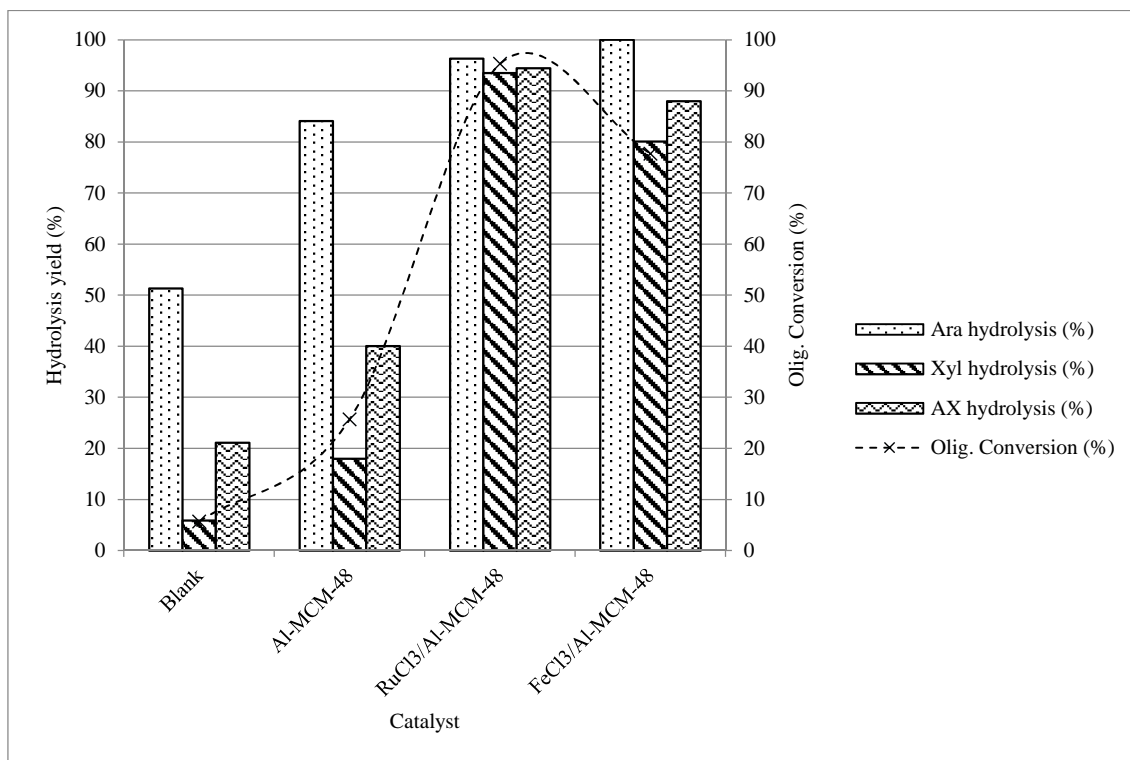
355

356 Fig. 5. Effect of time with high amount of catalyst in arabinoxylan hydrolysis. Reaction
 357 conditions: 180 °C, 50 bar N₂, catalyst: RuCl₃/Al-MCM-48, catalyst loading: 4.8 g catalyst·g C⁻¹
 358 in initial hemicelluloses. A) Hydrolysis yield of arabinoxylans into arabinose and xylose and
 359 oligomers conversion, B) Composition of the liquid after hydrolysis (g·L⁻¹).

360 3.3.3 Effect of cation (Ru⁺³, Fe⁺³)

361 The effect of different cations (Ru⁺³, Fe⁺³) was studied using RuCl₃ and FeCl₃ supported on Al-
 362 MCM-48 as catalysts. Experiments were performed at 180 °C, 15 minutes and 50 bar N₂ using
 363 4.8 g·g C⁻¹, which was optimized in previous sections. For comparison, a reaction with bare Al-
 364 MCM-48 was also carried out to point out the effect of the metal precursors. Results are shown
 365 in Fig. 6. It can be clearly seen that the incorporation of RuCl₃ or FeCl₃ enhances arabinoxylan
 366 hydrolysis. The hydrolysis of arabinose oligomers is almost complete with both supported
 367 catalysts. However, a higher hydrolysis yield of xylose oligomers is obtained with RuCl₃-
 368 catalyst, despite the greater acidity of FeCl₃/Al-MCM-48 (Table 2). Fe⁺³ and Ru⁺³ have been
 369 demonstrated to be active in hydrolysis of cellobiose and cellulose (Jing et al., 2016; Shimizu et
 370 al., 2009). Nevertheless, higher reaction rates were observed for catalysts with moderate Lewis

371 acidity, such as Ru^{+3} , than for those with high Lewis acidity, such as Fe^{+3} . This could explain
372 the better catalytic activity of RuCl_3 catalysts in comparison with FeCl_3 in arabinoxylan
373 hydrolysis (Shimizu et al., 2009).



374

375 Fig. 6. Effect of cation (Ru^{+3} , Fe^{+3}) in arabinoxylan hydrolysis and oligomers conversion.
376 Reaction conditions: 180 °C, 15 min, 50 bar N_2 , catalyst loading: 4.8 g catalyst·g C^{-1} in initial
377 hemicelluloses.

378 4. Conclusions

379 The use of heterogeneous catalysts has been demonstrated to be a good option for hydrolysis of
380 real arabinoxylans derived from wheat bran. The hydrolysis yield is improved by increasing the
381 acidity of the heterogeneous catalyst (MCM-48 < Al-MCM-48 < $\text{RuCl}_3/\text{MCM-48}$ < $\text{RuCl}_3/\text{Al-}$
382 MCM-48). Cations with moderate Lewis acidity (Ru^{+3}) present a higher activity in hydrolysis
383 processes than those with high Lewis acidity (Fe^{+3}). In this work, a high hydrolysis yield of
384 arabinoxylans into the corresponding monomers (94 and 96% for xylose and arabinose,
385 respectively) is achieved at 180 °C after 15 minutes using an amount of $\text{RuCl}_3/\text{Al-MCM-48}$
386 equal to 4.8 g·g⁻¹.

387 Acknowledgements

388 Authors gratefully acknowledge the financial support of Spanish Government through the
389 Research Project CTQ2015-64892-R (MINECO/FEDER). N. Sánchez-Bastardo thanks
390 Ministerio de Educación Cultura y Deporte for financial support through a FPU predoctoral
391 contract (FPU14/00812).

392 **References**

- 393 Aden, A., Ruth, M., Ibsen, K., Jechura, J., Neeves, K., Sheehan, J., Wallace, B., Montague, L.,
394 Slayton, A., Lukas, J., 2002. Lignocellulosic biomass to ethanol process design and economics
395 utilizing co-current dilute acid prehydrolysis and enzymatic hydrolysis for corn stover,
396 NREL/TP-510-32438.
- 397 Apprich, S., Tirpanalan, Ö., Hell, J., Reisinger, M., Böhmendorfer, S., Siebenhandl-Ehn, S.,
398 Novalin, S., Kneifel, W., 2014. Wheat bran-based biorefinery 2: Valorization of products. *LWT*
399 *Food Sci. Technol.* 56, 222-231.
- 400 Bandura, A.V., Lvov, S.N., 2006. The ionization constant of water over wide ranges of
401 temperature and density. *J. Phys. Chem. Ref. Data.* 35, 14-30.
- 402 Cará, P. D., Pagliaro, M., Elmekawy, A., Brown, D. R., Verschuren, P., Shiju, N. R.,
403 Rothenberg, G., 2013. Hemicellulose hydrolysis catalysed by solid acids. *Catal. Sci. Technol.* 3,
404 2057-2061.
- 405 Choudhary, H., Nishimura, S., Ebitani, K., 2013. Metal-free oxidative synthesis of succinic acid
406 from biomass-derived furan compounds using a solid acid catalyst with hydrogen peroxide.
407 *Appl. Catal., A.* 458, 55-62.
- 408 Dhepe, P. L., Sahu, R., 2010. A solid-acid-based process for the conversion of hemicellulose.
409 *Green Chem.* 12, 2153-2156.
- 410 Guisnet, M., Barbier, J., Barrault, J., Bouchoule, C., Duprez, D., Pérot, G., Montassier, C.,
411 1993. *Studies in Surface Science and Catalysis. Heterogeneous Catalysis and Fine Chemicals*
412 *III.* 1st Ed. Poitiers: Elsevier Science, 78, 1-719. Print ISBN 9780444890634.
- 413 Hendriks, A. T. W. M., Zeeman, G., 2009. Pretreatments to enhance the digestibility of
414 lignocellulosic biomass. *Bioresour. Technol.* 100, 10-18.

- 415 Hilpmann, G., Becher, N., Pahner, F-A., Kusema, B., Mäki-Arvela, P., Lange, R., Murzin, D.
416 Y., Salmi, T., 2016. Acid hydrolysis of xylan. *Catal. Today.* 259, 376-380.
- 417 Hu, H., Li, Z., Wu, Z., Lin, L., Zhou, S., 2016. Catalytic hydrolysis of microcrystalline and rice
418 straw-derived cellulose over a chlorine-doped magnetic carbonaceous solid acid. *Ind. Crops*
419 *Prod.* 84, 408-417.
- 420 Hu, L., Tang, X., Wu, Z., Lin, L., Xu, J., Xu, N., Dai, B., 2015. Magnetic lignin-derived
421 carbonaceous catalyst for the dehydration of fructose into 5-hydroxymethylfurfural in
422 dimethylsulfoxide. *Chem. Eng. J.* 263, 299-308.
- 423 Izydorczyk, M.S., Biliaderis, C.G., 2007. Arabinoxylans: Technologically and nutritionally
424 functional plant polysaccharides, in: Biliaderis, C. G., Izydorczyk, M. S. (Eds.), *Functional food*
425 *carbohydrates*. Boca Raton: CRC Press, pp. 249-290.
- 426 Jia, L., Budinova, G. A. L. G., Takasugi, Y., Noda, S., Tanaka, T., Ichinose, H., Goto, M.,
427 Kamiya, N., 2016. Synergistic degradation of arabinoxylan by free and immobilized xylanases
428 and arabinofuranosidase. *Biochem. Eng. J.* 114, 268-275.
- 429 Jing, S., Cao, X., Zhong, L., Peng, X., Zhang, X., Wang, S., Sun, R., 2016. In situ carbonic acid
430 from CO₂: A green acid for highly effective conversion of cellulose in the presence of Lewis
431 acid. *ACS Sustainable Chem. Eng.* 4, 4146-4155.
- 432 Kao, H-M., Chang, P-C., Liao, Y-W., Lee, L-P., Chien, C-H., 2008. Solid-state NMR
433 characterization of the acid sites in cubic mesoporous Al-MCM-48 materials using
434 trimethylphosphine oxide as a P NMR probe. *Microporous Mesoporous Mater.* 114, 352-364.
- 435 Kim, Y., Kreke, T., Ladisch, M. R., 2013. Reaction mechanisms and kinetics of xylo-
436 oligosaccharide hydrolysis by dicarboxylic acids. *AIChE Journal.* 59, 188-199.

- 437 Kobayashi, H., Komanoya, T., Guha, S.K., Hara, K., Fukuoka, A., 2011. Conversion of
438 cellulose into renewable chemicals by supported metal catalysis. *Appl. Catal., A.* 409-410, 13-
439 20.
- 440 Koganti, S., Ju, L-K., 2013. *Debaryomyces hansenii* fermentation for arabitol production.
441 *Biochem. Eng. J.* 79, 112-119.
- 442 Krithiga, T., Vinu, A., Ariga, K., Arabindoo, B., Palanichamy, M., Murugesan, V., 2005.
443 Selective formation 2,6-diisopropyl naphthalene over mesoporous Al-MCM-48 catalysts. *J.*
444 *Mol. Catal. A: Chem.* 237, 238-245.
- 445 Kusema, B. T., Hilmann, G., Mäki-Arvela, P., Willför, S., Holmbom, B., Salmi, T., Murzin, D.
446 Y., 2011. Selective hydrolysis of arabinogalactan into arabinose and galactose over
447 heterogeneous catalysts. *Catal. Lett.* 141, 408-412.
- 448 Kusema, B. T., Tönnov, T., Mäki-Arvela, P., Salmi, T., Willför, S., Holmbom, B., Murzin, D.
449 Y., 2013. Acid hydrolysis of O-acetyl-galactoglucomannan. *Catal. Sci. Technol.* 3, 116-122.
- 450 Lee, H. J., Kim, I. J., Kim, J. F., Choi, I-G., Kim, K. H., 2013. An expansin from the marine
451 bacterium *Hahella chejuensis* acts synergistically with xylanase and enhances xylan hydrolysis.
452 *Bioresour. Technol.* 149, 516–519.
- 453 Li, F., Wang, H., Xin, H., Cai, J., Fu, Q., Jin, Y., 2016. Development, validation and application
454 of a hydrophilic interaction liquid chromatography-evaporative light scattering detection based
455 method for process control of hydrolysis of xylans obtained from different agricultural wastes.
456 *Food Chem.* 212, 155-161.
- 457 Li, H., Xue, Y., Wu, J., Wu, H., Qin, G.; Li, C., Ding, J., Liu, J., Gan, L., Long, M., 2016.
458 Enzymatic hydrolysis of hemicelluloses from *Miscanthus tomonosaccharides* or xylo-
459 oligosaccharides by recombinant hemicellulases. *Ind. Crops Prod.* 79, 170-179.

- 460 Liu, W-J., Tian, K., Jiang, H., Yu, H-Q., 2013. Facile synthesis of highly efficient and
461 recyclable magnetic solid acid from biomass waste. *Sci. Rep.* 3, 2419.
- 462 Lou, H., Yuan, L., Qiu, X., Qiu, K., Fu, J., Pang, Y., Huang, J., 2016. Enhancing enzymatic
463 hydrolysis of xylan by adding sodium lignosulfonate and long-chain fatty alcohols. *Bioresour.*
464 *Technol.* 200, 48–54.
- 465 Moreira, L. R. S., Filho, E. X. F., 2016. Insights into the mechanism of enzymatic hydrolysis of
466 xylan. *Appl. Microbiol. Biotechnol.* 100, 5205-5214.
- 467 Nakasu, P. Y. S., Ienczak, L. J., Costa, A. C., Rabelo, S.C., 2016. Acid post-hydrolysis of
468 xylooligosaccharides from hydrothermal pretreatment for pentose ethanol production. *Fuel.* 185,
469 73-84.
- 470 Negahdar, L., Delidovich, I., Palkovits, R., 2016. Aqueous-phase hydrolysis of cellulose and
471 hemicelluloses over molecular acidic catalysts: Insights into the kinetics and reaction
472 mechanism. *Appl. Catal., B.* 184, 285-298.
- 473 Oh, Y. H., Eom, I. Y., Joo, J. C., Yu, J. H., Song, B. K., Lee, S. H., Hong, S. H., Park, S. J.,
474 2015. Recent advances in development of biomass pretreatment technologies used in
475 biorefinery for the production of bio-based fuels, chemicals and polymers. *Korean J. Chem.*
476 *Eng.* 32, 1945.
- 477 Ormsby, R., Kastner, J. R., Miller, J., 2012. Hemicellulose hydrolysis using solid acid catalysts
478 generated from biochar. *Catal. Today.* 190, 89- 97.
- 479 Prückler, M., Siebenhandl-Ehn, S., Apprich, S., Höltinger, S., Haas, C., Schmid, E., Kneifel,
480 W., 2014. Wheat bran-based biorefinery 1: Composition of wheat bran and strategies of
481 functionalization. *LWT Food Sci. Technol.* 56, 211-221.
- 482 Putro, J. N., Soetaredjo, F. E., Lin, S-Y., Ju, Y-H., Ismadji, S., 2016. Pretreatment and
483 conversion of lignocellulose biomass into valuable chemicals. *RSC Adv.* 6, 46834-46852.

484 Romero, A., Alonso, E., Sastre, Á., Nieto-Márquez, A., 2016. Conversion of biomass into
485 sorbitol: cellulose hydrolysis on MCM-48 and D-glucose hydrogenation on Ru/MCM-48.
486 Microporous Mesoporous Mater. 224, 1-8.

487 Sahu, R., Dhepe, P.L., 2012. A one-pot method for the selective conversion of hemicellulose
488 from crop waste into C5 sugars and furfural by using solid acid catalysts. ChemSusChem. 5,
489 751-761.

490 Salmi, T., Murzin, D., Wärna, J., Mäki-Arvela, P., Kusema, B., Holmbom, B., Willför, S., 2014.
491 Hemicellulose hydrolysis in the presence of heterogeneous catalysts. Topics in Catalysis. 57,
492 1470-1475.

493 Sánchez-Bastardo, N., Romero, A., Alonso, E., 2017. Extraction of arabinoxylans from wheat
494 bran using hydrothermal processes assisted by heterogeneous catalysts. Carbohydr. Polym. 160,
495 143-152.

496 Shimizu, K-I., Furukawa, H., Kobayashi, N., Itaya, Y., Satsuma, A., 2009. Effects of Brønsted
497 and Lewis acidities on activity and selectivity of heteropolyacid-based catalysts for hydrolysis
498 of cellobiose and cellulose. Green Chem. 11, 1627-1632.

499 Singhvi, M. S., Chaudhari, S., Gokhale, D. V., 2014. Lignocellulose processing: a current
500 challenge. RSC Adv. 4, 8271.

501 Sluiter, A., Hames, B., Ruiz, R., Scarlata, C., Sluiter, J., Templeton, D., 2008. Determination of
502 Sugars, Byproducts, and Degradation Products in Liquid Fraction Process Samples. Laboratory
503 Analytical Procedure (LAP). Technical Report NREL/TP-510-42623.

504 Tathod, A., Kane, T., Sanil, E. S., Dhepe, P. L., 2014. Solid base supported metal catalysts for
505 the oxidation and hydrogenation of sugars. J. Mol. Catal. A: Chem. 388-389, 90-99.

506 Vilcocq, L., Castilho, P. C., Carvalheiro, F., Duarte, L. C., 2014. Hydrolysis of oligosaccharides
507 over solid acid catalysts: A review. ChemSusChem. 7, 1010-1019.

- 508** Wang, J., Xu, W., Ren, J., Liu, X., Lu, G., Wang, Y., 2011. Efficient catalytic conversion of
509 fructose into hydroxymethylfurfural by a novel carbon-based solid acid. *Green Chem.* 13, 2678-
510 2681.
- 511** Xue, P., Lu, G., Guo, Y., Wang, Y., Guo, Y., 2004. A novel support of MCM-48 molecular
512 sieve for immobilization of penicillin G acylase. *J. Mol. Catal. B: Enzym.* 30, 75-81.
- 513** Zhang, J., Zhuang, J., Lin, L., Liu, S., Zhang, Z., 2012. Conversion of D-xylose into furfural
514 with mesoporous molecular sieve MCM-41 as catalyst and butanol as the extraction phase.
515 *Biomass Bioenergy.* 39, 73-77.
- 516** Zheng, F-C., Chen, Q-W., Hu, L., Yan, N., Kong, X-K., 2014. Synthesis of sulfonic acid-
517 functionalized Fe₃O₄@C nanoparticles as magnetically recyclable solid acid catalysts for
518 acetalization reaction. *Dalton Trans.* 43, 1220-1227.
- 519** Zhou, L., Shi, M., Cai, Q., Wu, L., Hu, X., Yang, X., Chen, C., Xu, J., 2013. Hydrolysis of
520 hemicellulose catalyzed by hierarchical H-USY zeolites – The role of acidity and pore structure.
521 *Microporous Mesoporous Mater.* 169, 54-59.